THE JOURNAL OF BIOLOGICAL CHEMISTRY VOL. 288, NO. 14, pp. 9602–9609, April 5, 2013

A Periodic Pattern of Evolutionarily Conserved Basic and Acidic Residues Constitutes the Binding Interface of Actin-Tropomyosin*

Received for publication, January 7, 2013, and in revised form, February 11, 2013 Published, JBC Papers in Press, February 18, 2013, DOI 10.1074/jbc.M113.451161

Bipasha Barua[‡§1], Patricia M. Fagnant[¶], Donald A. Winkelmann[§], Kathleen M. Trybus[¶], and Sarah E. Hitchcock-DeGregori[‡§]

From the Departments of [‡]Neuroscience and Cell Biology and [§]Pathology and Laboratory Medicine, Robert Wood Johnson Medical School, Piscataway, New Jersey 08854 and [¶]Department of Molecular Physiology and Biophysics, University of Vermont, Burlington, Vermont 05405

Background: The interface of actin with tropomyosin, the universal regulator of the actin filament, is unknown.
Results: Mutagenesis of actin and tropomyosin revealed a pattern of residues required for complex formation in the closed state.
Conclusion: The results support models of the actin-tropomyosin filament in the absence of myosin and troponin.
Significance: A validated actin-tropomyosin model is required to understand regulation and disease mechanisms.

Actin filament cytoskeletal and muscle functions are regulated by actin binding proteins using a variety of mechanisms. A universal actin filament regulator is the protein tropomyosin, which binds end-to-end along the length of the filament. The actin-tropomyosin filament structure is unknown, but there are atomic models in different regulatory states based on electron microscopy reconstructions, computational modeling of actin-tropomyosin, and docking of atomic resolution structures of tropomyosin to actin filament models. Here, we have tested models of the actin-tropomyosin interface in the "closed state" where tropomyosin binds to actin in the absence of myosin or troponin. Using mutagenesis coupled with functional analyses, we determined residues of actin and tropomyosin required for complex formation. The sites of mutations in tropomyosin were based on an evolutionary analysis and revealed a pattern of basic and acidic residues in the first halves of the periodic repeats (periods) in tropomyosin. In periods P1, P4, and P6, basic residues are most important for actin affinity, in contrast to periods P2, P3, P5, and P7, where both basic and acidic residues or predominantly acidic residues contribute to actin affinity. Hydrophobic interactions were found to be relatively less important for actin binding. We mutated actin residues in subdomains 1 and 3 (Asp^{25}-Glu^{334}-Lys^{326}-Lys^{328}) that are poised to make electrostatic interactions with the residues in the repeating motif on tropomyosin in the models. Tropomyosin failed to bind mutant actin filaments. Our mutagenesis studies provide the first experimental support for the atomic models of the actin-tropomyosin interface.

Tropomyosin (Tm)[2] is a regulator of the actin cytoskeleton that is involved in diverse cellular functions, including muscle contraction, cytokinesis, intracellular transport, and cell migration (1–3). Tropomyosin is a two-chained α-helical coiled coil protein that associates end-to-end to form continuous strands on both sides of the actin filament. Binding of Tm to actin regulates the stability and functions of actin filaments in most eukaryotic muscle and non-muscle cells ranging from mammals to fungi. In striated muscle, Tm and troponin regulate muscle contraction by Ca^{2+}-dependent regulation of the binding of myosin heads (myosin S1) to actin filaments. Mutations in Tm cause skeletal and cardiomyopathies (4, 5). In non-muscle cells, Tm regulates actin filament dynamics as well as interaction of actin with actin binding proteins, including myosin, tropomodulin, formin, Arp2/3, and ADF-cofilin (1, 3). Elimination of both tropomyosin genes in budding yeast is lethal (1). Although the ability to bind actin filaments is a universal function of Tm, the specific residues of actin and Tm that constitute the binding interface of the actin-Tm complex remain unknown.

Striated muscle αTm spans the length of seven actin monomers in the actin filament and was proposed to have seven quasi-equivalent periodic repeats (periods, P1–P7) with a pattern of residues within each period postulated to be actin binding sites (6, 7). Subsequent biochemical and biophysical studies defined features of the Tm molecule that are important for actin binding and regulation, including the molecular ends, an uninterrupted heptad repeat, regions of local instability at the coiled coil interface characterized by the presence of small nonpolar residues such as Ala, and a sequence pattern on the surface of the coiled coil that was proposed as a recognition site for actin binding (8–11). Previous studies have also shown that individual periodic repeats of Tm contribute in different ways to actin binding and regulatory function (11–15). Atomic models based on electron microscopy (EM) reconstructions, three-dimensional fluorescence resonance energy transfer (FRET) analysis and computational modeling of actin-Tm have revealed the positions of Tm on the actin filament in the absence and presence of troponin ± Ca^{2+}, and myosin S1 (16–19). However, there is no high-resolution, residue-specific

* This work was supported by National Institutes of Health Grants GM093065 (to S. E. H.-D.) and HL110869 (to K. M. T.).
[1] To whom correspondence should be addressed: Dept. of Neuroscience and Cell Biology, Robert Wood Johnson Medical School, 675 Hoes Ln., Piscataway, NJ 08854. Tel.: 732-235-4528; Fax: 732-235-4029; E-mail: baruabi@umdnj.edu.
[2] The abbreviations used are: Tm, tropomyosin(s); myosin S1, myosin subfragment 1; T_M, melting temperature.

structural information available for the actin-Tm binding interface.

We previously reported an evolutionary analysis of Tm from 26 species ranging from cnidarians to vertebrates and determined the evolutionarily conserved residues of Tm (20). Evolutionarily conserved residues at *b*, *c*, or *f* surface positions of the coiled coil heptad repeat of Tm were mutated to Ala within the first half or the second half of periods P2–P6. All Tm mutations, except one, were at charged residues, indicating that binding is primarily electrostatic in nature. Mutations in the first half of P2 (P2-1-KDDE), P4 (P4-1-RKV), and P5 (P5-1-REEE) showed the largest reduction in actin affinity (>4-fold), inferring that these mutations include residues in actin-binding sites. A structural model constructed to assess the structural relevance of these mutations showed potential periodic interactions of mutated sites in Tm with residues in subdomains 1 and 3 of successive actin monomers of the filament and is consistent with other models (18, 21). Mutations in the second halves of the periods primarily affect actomyosin regulation (22).

In the present work, we refined our analysis of conserved surface residues (20) to determine features of individual periods that form actin binding sites on Tm. In addition, we extended the analysis to include periods P1 and P7. Our goal was to determine the actin-tropomyosin interface residues in the absence of proteins such as troponin and myosin that modify the intrinsic actin affinity of tropomyosin. We determined that actin binding sites on Tm follow an alternating pattern of basic and basic-acidic residues in each periodic repeat. In P1, P4, and P6, basic residues are most important for actin affinity, in contrast to P2, P3, P5, and P7, where both basic and acidic residues or mostly acidic residues contribute to actin affinity. Hydrophobic interactions are relatively less important for actin binding. To test the models of the actin-Tm interface (18, 20, 21), we mutated actin residues in subdomains 1 and 3 (Asp^{25}-Glu^{334}-Lys^{326}-Lys^{328}) that are poised to make electrostatic interactions with the residues in the repeating motif on Tm. Tropomyosin failed to bind mutant actin filaments, in support of the models. The velocity of the mutant actin filament was reduced in an actomyosin motility assay, suggesting that these residues are also involved in actin-myosin interaction.

EXPERIMENTAL PROCEDURES

DNA Construction and Protein Purification—Mutations were made in rat striated α-tropomyosin cDNA with an Ala-Ser extension at the N terminus, cloned in pET11d for expression in *Escherichia coli* (23). Recombinant AS-αTm binds well to actin in the absence of troponin, unlike recombinant unacetylated-αTm. Mutations were made using oligonucleotides and their reverse complements using two-stage PCR as described previously (9). The mutations were verified by sequencing of the DNA at the DNA Core Facility at Robert Wood Johnson Medical School and Genewiz. Mutants were expressed in *E. coli* BL21(DE3) cells and purified as described previously (9). Actin was purified from acetone powder of chicken pectoral skeletal muscle actin (24). Tm and actin concentrations were determined by measuring the difference spectrum of tyrosine (9). The molecular weights of the purified proteins were verified by electrospray mass spectrometry at the Keck Biotechnology Resource Lab (Yale University).

Smooth Muscle Actins—Recombinant baculovirus were prepared according to established protocols (25). Human vascular smooth muscle actins (*ACTA2*) were tagged at the C terminus with a His_6, using the method described in Noguchi *et al.* (26). Infected Sf9 cells were harvested after 72 h and lysed in 1 M Tris-HCl, pH 7.5 at 4 °C, 0.6 M KCl, 0.5 mM $MgCl_2$, 4% Triton X-100, 1 mg/ml Tween 20, 0.5 mM Na_2ATP, 1 mM DTT, 0.5 mM 4-(2-aminoethyl)-benzenesulfonyl fluoride hydrochloride, 5 mM benzamidine, and 5 μg/ml leupeptin for 2.5 h (40 ml/1 billion cells). After clarification at 178,000 × *g* for 45 min, the supernatant was dialyzed overnight into 10 mM HEPES, pH 7.5, 0.3 M NaCl, 0.2 mM $CaCl_2$, 0.25 mM Na_2ATP, 7 mM β-mercaptoethanol, and 1 μg/ml leupeptin. The dialysate was clarified at 25,000 × *g* for 30 min and then incubated with His-Select Nickel Affinity Gel (Sigma). The column was washed first with the dialysis buffer without imidazole and then with the dialysis buffer containing 10 mM imidazole. Protein was eluted with dialysis buffer containing 50 mM imidazole. Pure fractions were combined, concentrated using an Amicon concentrator, and dialyzed into G buffer (5 mM Tris, pH 8.26 at 4 °C, 0.2 mM $CaCl_2$, 0.1 mM NaN_3, 0.5 mM DTT, 0.2 mM Na_2ATP, 1 μg/ml leupeptin). The tag was cleaved off of the actin, and the tag was separated from actin on a MonoQ column, essentially as described in Noguchi *et al.* (26). Pure actin was dialyzed against G-buffer for 2 days, clarified, and polymerized by the addition of 2 mM $MgCl_2$ and 0.1 mM KCl.

Actin Binding Assays—Tropomyosin (0.1–8 μM) was combined with 5 μM chicken skeletal F-actin or 3 μM human vascular smooth F-actin and cosedimented at 20 °C in 200 mM NaCl, 10 mM Tris-HCl, pH 7.5, 2 mM $MgCl_2$, and 0.5 mM DTT at 60,000 rpm in a Beckman model TL-100 ultracentrifuge in a TLA-100 rotor (27). The pellets and supernatants were analyzed by SDS-PAGE, stained with Coomassie Blue, and scanned and analyzed using ImageScanner III densitometer with Labscan (version 6.0) and ImageQuant TL (version 7.0) image analysis software. The free Tm in the supernatants was calculated from standard curves for WT-Tm. The binding constant K_{app} and the Hill coefficient (αH) were determined by fitting the experimental data to the Hill equation (Equation 1) (9) using Kaleidagraph,

$$\nu = (n[\mathrm{Tm}]^{\alpha H}K_{app}{}^{\alpha H})/(1 + [\mathrm{Tm}]^{\alpha H}K_{app}{}^{\alpha H}) \qquad \text{(Eq. 1)}$$

where ν = fraction maximal Tm binding to actin, n = maximal Tm bound, and $[\mathrm{Tm}] = [\mathrm{Tm}]_{free}$. The Tm:actin ratio was normalized to 1 by dividing the Tm:actin ratio obtained from densitometry by the Tm:actin ratio observed at saturation.

Circular Dichroism (CD) Measurements—Thermal stability measurements were made by following the ellipticity of 1.5 μM Tm at 222 nm as a function of temperature in 0.5 M NaCl, 10 mM sodium phosphate, pH 7.5, 1 mM EDTA, and 1 mM DTT in an Aviv model 400 spectropolarimeter at the Robert Wood Johnson Medical School CD facility. The observed melting temperature (T_M) is defined as the temperature at which the ellipticity at 222 nm, normalized to a scale of 0 to 1, is equal to 0.5 (28).

EM Imaging—Actin was diluted to 15 μg/ml in 10 mM Tris, pH 7.5, 2 mM $MgCl_2$, 0.5 mM DTT, 100 mM NaCl, and 0.1 mM

ATP and applied to freshly prepared carbon-coated butvar grids and negatively stained with 1% uranyl acetate in water. Images were recorded with a Phillips CM12 transmission electron microscope operating at 80 kV and 45,000× magnification with an AMT XR611 digital system.

In Vitro Motility Assays—The *in vitro* motility assays were done as described in (22, 29). Nitrocellulose-coated glass coverslips were incubated with 0.15 mg/ml of a monoclonal antibody that reacts specifically with myosin subfragment 2 (anti-S2 mAb, 10F12.3), followed by incubation with 1% BSA for blocking. Myosin was diluted in 25 mM imidazole, pH 7.6, 0.3 M KCl, 4 mM $MgCl_2$, 5 mM DTT supplemented with 1% BSA to a final concentration of 40 μg/ml. The antibody-coated coverslips were incubated with 40 μg/ml myosin for ~2 h in a humidified chamber at 4 °C. The coverslips were washed with motility buffer (25 mM imidazole, pH 7.6, 25 mM KCl, 4 mM $MgCl_2$, 1 mM MgATP, 5 mM DTT), then transferred to a 15-μl drop of 2 nM rhodamine phalloidin-labeled smooth muscle WT or mutant actin in a modified motility buffer (25 mM imidazole, pH 7.6, 25 mM KCl, 4 mM $MgCl_2$, 7.6 mM MgATP, 50 mM DTT, 0.5% methyl cellulose, 0.1 mg/ml glucose oxidase, 0.018 mg/ml catalase, 2.3 mg/ml glucose) in a small parafilm ring fixed on an alumina slide with vacuum grease. This chamber was observed with an Olympus BH-2 microscope. The movement of actin filaments from 1–2 min of continuous video was recorded from several fields for each assay condition and analyzed with semi-automated filament tracking programs as described previously (22, 30, 31).

RESULTS

Tropomyosin Mutant Design—In a previous study, evolutionarily conserved residues of Tm at surface *b*, *c*, or *f* heptad repeat positions in periods P2–P6 were mutated to alanine with three to four residues mutated in each construct in a 284-residue rat striated αTm with a N-terminal Ala-Ser extension to mimic acetylation (20). The Ala-Ser Tm functions normally in *in vitro* analyses as well as in reconstituted fibers (23, 32, 33). Here, we have carried out further mutagenesis to determine the contribution of individual residues within the first half of periods P1–P7 to actin binding to refine our understanding of the actin binding sites on the surface of Tm. The additional mutations are all of well conserved sites and include single-site mutations and tests of the importance of the pattern of conserved surface residues. A pattern of basic and acidic surface residues is conserved in the first half of P1–P7 at positions *f*, *b*, and *f* of the heptad repeat (shown by the *blue* and *red boxes* in Fig. 1). At the first *f* position (*blue box*, Fig. 1), there is a basic residue (Lys^6, Lys^{48}, Arg^{90}, Arg^{125}, Arg^{167}, and Arg^{244}) in each period except P6 (Ala^{209}). However in P6, there are two basic residues at adjacent *b* and *c* positions (Lys^{205} and Lys^{213}) that may be analogous to the basic residues at position *f*. At the *b* and *f* positions C-terminal to the basic residues (*red boxes*, Fig. 1), there are acidic residues in all periods except position *b* in P4 (Gln^{135}).

Here, we have introduced the following mutations: the basic and acidic residues at the *f*, *b*, *f* positions in P1 and P7 were mutated to Ala, the R90A and D100A mutations were added to the P3–1-EE mutant, and the K205A, D219A, and E223A mutations were added to the K213A (P6–1-K) mutant (20) (Fig. 1).

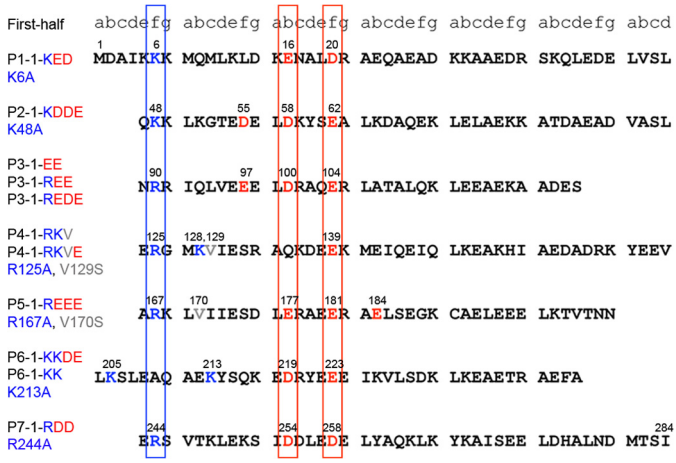

FIGURE 1. **Tropomyosin mutations at conserved surface residues.** The rat striated αTm sequence showing conserved *b*, *c*, and *f* residues that were mutated to Ala in the first half of periods P1–P7. The names of the mutants on the *left* indicate the basic (*blue*), acidic (*red*), or hydrophobic (*gray*) residues that were mutated in the first half (1) of each period (P1–P7). The pattern of basic and acidic residues at positions *f*, *b*, and *f* are indicated by the *blue* (position *f*, basic residues) and *red* (positions *b* and *f*, acidic residues) *boxes*.

We carried out single residue mutations to Ala at the basic residues in position *f*: Lys^6, Lys^{48}, Arg^{125}, Arg^{167}, and Arg^{244}, and at Lys^{205}–Lys^{213} in P6 (P6–1-KK), to separate the contributions of basic and acidic residues to actin affinity. We also mutated hydrophobic residues in P4 (Val^{129}) and P5 (Val^{170}) to serine to test the contribution of hydrophobic interactions to actin binding.

Actin Affinity of Tropomyosins—The actin affinity (K_{app}) of the Tm mutants was determined by cosedimentation with skeletal muscle F-actin (Fig. 2, Table 1). All mutations reduced actin affinity >2-fold. The reduction in actin affinity caused by a mutation, either individual or in combination with others, was taken to indicate the contribution of that residue to an actin binding site on Tm. Mutations of non-conserved residues in these regions, or conserved residues in the second halves of the periods have little to no effect on actin affinity (20). The P4-1-RKVE and P4-1-RKV mutants have similar actin affinities, indicating that the E139A mutation does not affect actin binding.

The loss in affinity shown by basic residue mutants in P1 (K6A), P4 (R125A), and P6 (P6-1-KK) was similar to that of the basic-acidic residue mutants (P1-1-KED, P4-1-RKV, and P6-1-KKDE) indicating the actin binding sites in P1, P4, and P6 are primarily the basic residues. In contrast, basic residue mutations in P2 (K48A), P3 (P3-1-REE), P5 (R167A), and P7 (R244A) accounted for about half or less than half of the loss in affinity shown by the basic-acidic residue mutants (P2-1-KDDE, P3–1-REDE, P5-1-REEE, and P7-1-RDD), indicating the contribution of both basic and acidic residues to actin binding in these periods. A mutant with four basic residues mutated (K48A/R90A/R125A/R167A) had ~7-fold decrease in affinity similar to R125A confirming that Arg^{125} has the largest contribution to actin affinity among the four mutated basic residues. Mutation of hydrophobic residues in P4 (V129S) and P5 (V170S) had a ~2–3-fold effect on actin affinity, indicating the relatively smaller contribution of hydrophobic interactions to actin bind-

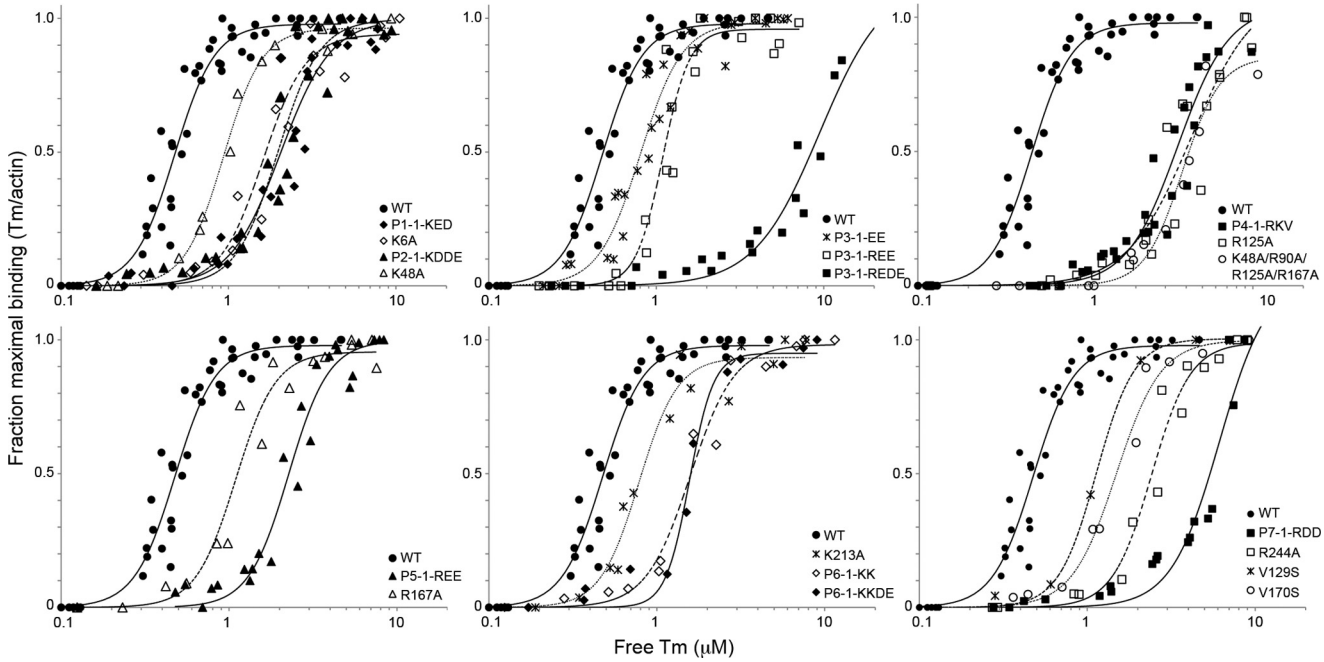

FIGURE 2. **Actin affinity of tropomyosin mutants measured by cosedimentation with F-actin.** Tropomyosin (0.1–8 μM) was combined with 5 μM chicken skeletal α-actin and sedimented at 20 °C in 200 mM NaCl, 10 mM Tris-HCl (pH 7.5), 2 mM $MgCl_2$, and 0.5 mM DTT. Stoichiometric binding of one Tm per seven actins is represented by fraction maximal binding of 1. The data for each mutant and WT were obtained from two to six independent experiments. The K_{app} values are reported in Table 1.

TABLE 1

Actin affinity and T_M from the ellipticity at 222 nm (CD) of tropomyosin mutants

Mutant	K_{app}[a]	K_{WT}/K_{mut}	CD[b] T_M
	$\times 10^6$ M^{-1}		°C
WT[c]	2.1 ± 0.1		49
K6A	0.6 ± 0.0	4	49
P1-1-KED	0.5 ± 0.0	4	49
K48A	1.1 ± 0.0	2	49
P2-1-KDDE[c]	0.5 ± 0.0	4	49
P3-1-EE[c]	1.2 ± 0.1	2	49
P3-1-REE	0.9 ± 0.0	2	49
P3-1-REDE	0.1 ± 0.0	>10	48
R125A	0.2 ± 0.1	10	48
P4-1-RKV[c]	0.3 ± 0.0	7	47
P4-1-RKVE[c]	0.4 ± 0.0	5	49
R167A	0.9 ± 0.1	2	47
P5-1-REEE[c]	0.4 ± 0.0	5	51
K213A (P6-1-K)	1.3 ± 0.1	2	49[c]
P6-1-KK	0.6 ± 0.0	4	49
P6-1-KKDE	0.6 ± 0.0	4	51
P7-1-RDD	0.2 ± 0.0	10	52
R244A	0.4 ± 0.0	5	49
48A/90A/125A/167A	0.3 ± 0.0	7	47
V129S	0.9 ± 0.0	2	49
V170S	0.7 ± 0.0	3	49

[a] The values for K_{app} shown with S.E. The data were fit to the Hill equation, and the K_{app} values are those reported by Kaleidagraph.
[b] T_M is the temperature at which the ellipticity at 222 nm, normalized to a scale of 0 to 1, is equal to 0.5.
[c] The K_{app} and T_M values are from Barua *et al.* (20).

ing. These results indicate that the binding interface of actin-Tm is primarily electrostatic in nature and the actin binding sites on Tm alternate between basic residues and basic-acidic residues in each period (see Fig. 6).

Thermal Stability of Tropomyosins—The thermal unfolding of the Tm α-helical coiled coil was determined using CD by measuring the ellipticity at 222 nm from 0–65 °C. The thermal unfolding data did not show any major change in the stability of the Tm mutants compared with WT (Table 1, Fig. 3). The overall melting temperature (T_M, temperature at which tropomyosin is 50% unfolded) of the mutants was within 2–3 °C of WT T_M. Previous studies have shown that stabilization of interface regions of Tm that contain Ala and other destabilizing residues leads to decreased actin affinity. There is no correlation between the reduced actin affinities of our mutants and the small changes in thermal stability, allaying concern that the Ala mutations may affect actin affinity because of changes in the global stability of the Tm. The small effect of the mutations on T_M indicates that there is no global stabilization, implying that the reduced actin affinity of mutants reflects binding specificity and is not a consequence of helical stabilization.

Smooth Muscle Actins—EM and computational models of the actin-tropomyosin complex suggest that the binding sites for Tm on actin are in subdomains 1 and 3. Based on the results with Tm mutants in this and our previous study and models of actin-Tm (18, 20, 21), we hypothesize that the pattern of basic and acidic residues in the first halves of periodic repeats of Tm interact with oppositely charged residues, Asp^{25}, Glu^{334}, Lys^{326}, and Lys^{328}, of actin (Fig. 4). To test this, we made an actin mutant, D25A/E334A/K326A/K328A, with four residues mutated to Ala. The mutations were made in a human vascular smooth muscle α-actin (*ACTA2*) construct and expressed in *Drosophila* Sf9 cells. EM of negatively stained samples of actin showed normal actin filament morphology for both WT and D25A/E334A/K326A/K328A smooth muscle actins (Fig. 5*A*).

The binding of WT and D25A/E334A/K326A/K328A actin to WT Tm was measured by cosedimentation (Fig. 5*B* and Table 2). WT actin bound to WT Tm with a binding constant (K_{app}) of 7×10^6 M^{-1}. In contrast, the D25A/E334A/K326A/K328A mutant did not show measurable binding to WT Tm, implying that one or more of the mutated actin residues contain

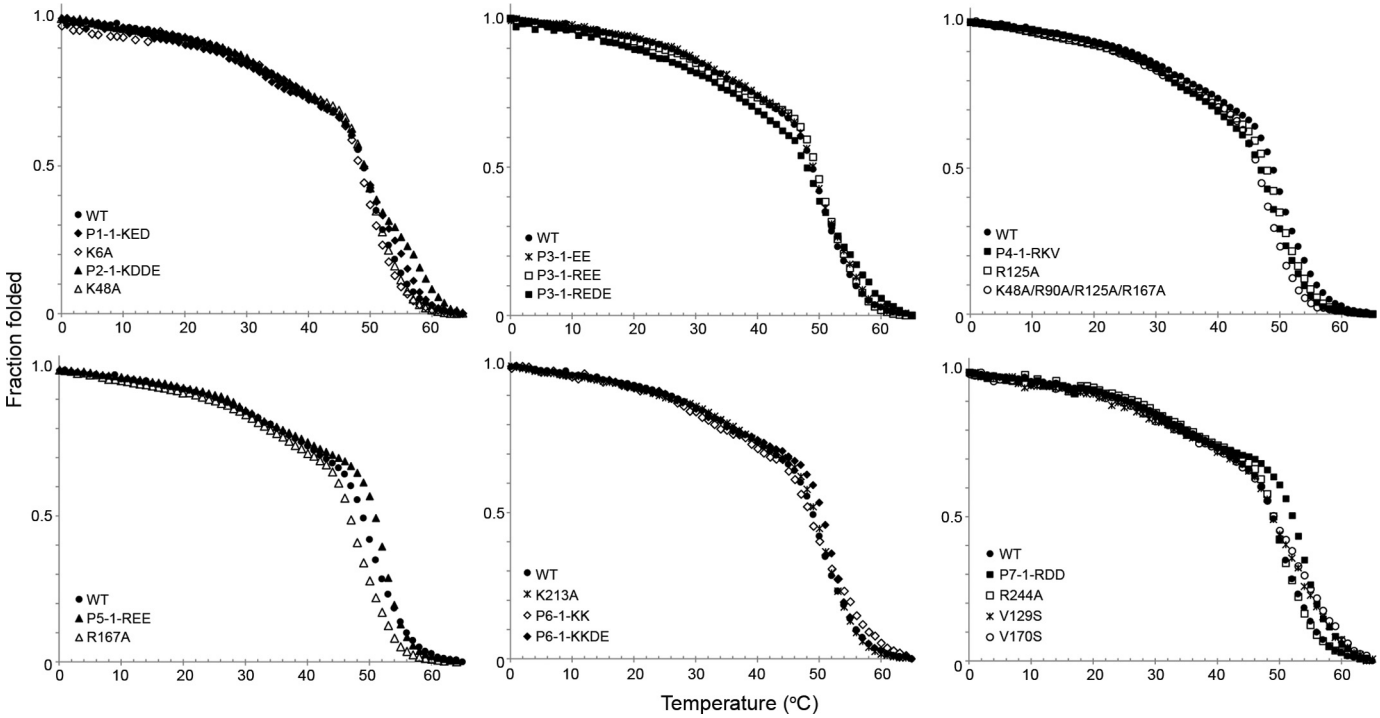

FIGURE 3. **Thermal stability of Tm mutants measured by circular dichroism.** Fraction folded as measured by relative ellipticity at 222 nm as a function of temperature. The Tm concentration was 1.5 μM in 0.5 M NaCl, 10 mM sodium phosphate (pH 7.5), 1 mM EDTA, and 1 mM DTT. The fraction folded is relative to the mean residue ellipticity at 0 °C, where the proteins were fully folded. The T_M values are reported in Table 1.

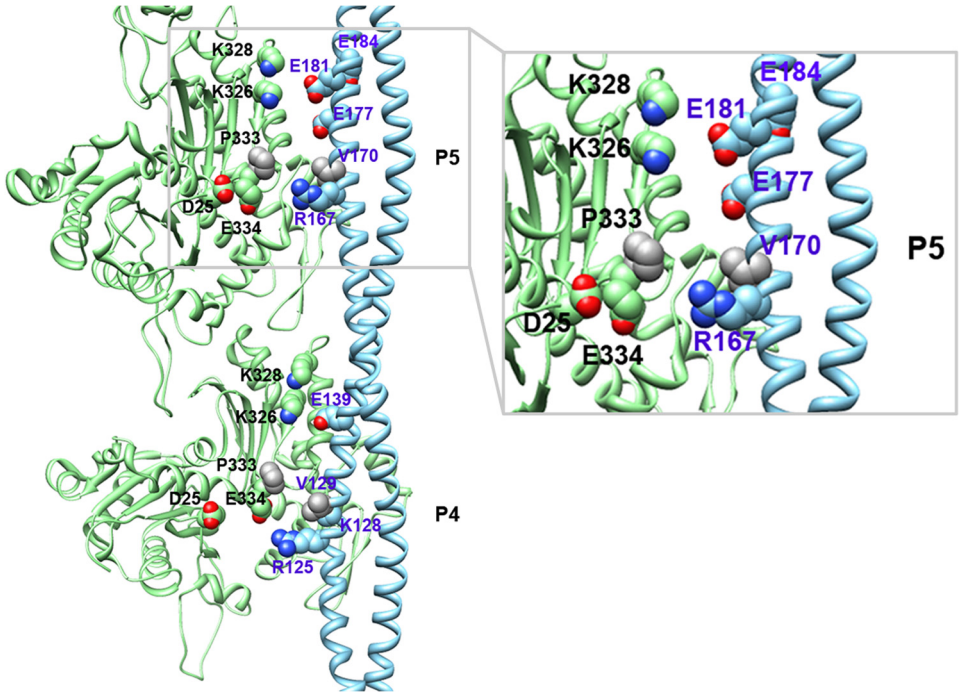

FIGURE 4. **Model for actin-tropomyosin interaction.** The model was constructed by docking a 2.3 Å Tm crystal structure (*blue*, Protein Data Bank code 2B9C) (21) including periods P4 and P5, and a 6.6 Å F-actin structure (*green*, Protein Data Bank code 3MFP) (47) as described in Barua *et al.* (20). The model shows potential electrostatic and hydrophobic interactions between Tm residues in P4 and P5 and actin residues. The zoomed portion shows the actin-Tm interface in P5. The model was constructed using the University of California, San Francisco Chimera package (48).

a binding site for Tm. The filament speeds of WT and D25A/E334A/K326A/K328A actin were determined using *in vitro* motility assays on skeletal myosin surfaces at a myosin density that allows maximal velocity of skeletal actin filaments (Fig. 5*C* and Table 2). The velocity of D25A/E334A/K326A/K328A was ~25% slower relative to WT actin and the fraction of moving filaments decreased from ~80% for WT to ~35% for D25A/E334A/K326A/K328A actin. These results indicate that the actin mutations may impair myosin binding and/or ATPase activation.

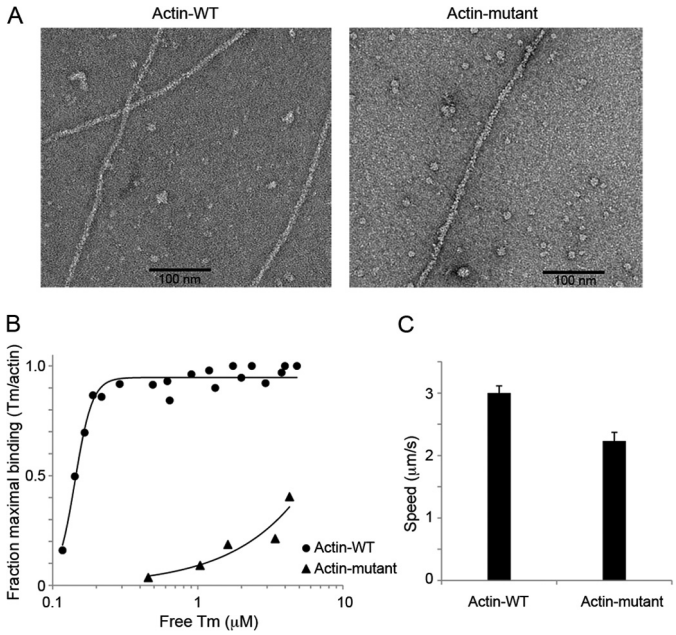

FIGURE 5. **Smooth muscle WT and D25A/E334A/K326A/K328A (mutant) α-actins.** *A*, EM images of F-actin negatively stained with uranyl acetate. *B*, affinity of actins for WT Tm measured by cosedimentation assay. Tropomyosin (0.1–8 μM) was combined with 3 μM F-actin and sedimented at 20 °C in 200 mM NaCl, 10 mM Tris-HCl (pH 7.5), 2 mM $MgCl_2$, and 0.5 mM DTT. The K_{app} values are reported in Table 2. *C*, filament speed of actins in *in vitro* motility assays. The values are mean ± S.D. from two experiments. An anti-myosin subfragment 2 monoclonal antibody was bound to nitrocellulose-coated glass coverslips and then incubated with 40 μg/ml chicken skeletal myosin at 4 °C for 2 h. The coverslips were transferred to 15-μl drops of 2 nM rhodamine-phalloidin labeled smooth muscle F-actins in motility buffer (25 mM imidazole, pH 7.6, 25 mM KCl, 4 mM $MgCl_2$, 7.6 mM MgATP, 50 mM DTT, 0.5% methyl cellulose), and an oxygen scavenger system (0.1 mg/ml glucose oxidase, 0.02 mg/ml catalase, 2.5 mg/ml glucose) and 1–2 min of continuous video of movement of actin filaments were recorded from several fields for each experiment at 27 °C.

TABLE 2

Tropomyosin binding affinity and filament speeds of actin

ND indicates that K_{app} was not measurable, $<0.01 \times 10^6\ M^{-1}$.

Smooth muscle actin	K_{app}[a]	Speed[b]	% Moving/Total no.[c]
	$\times 10^6\ M^{-1}$	μm/s	
WT	7.0 ± 0.1	3.0 ± 0.1	81/163
D25A/E334A/K326A/K328A	ND	2.2 ± 0.1	34/178

[a] The values for K_{app} shown with S.E. The data were fit to the Hill equation, and the K_{app} values are those reported by Kaleidagraph.
[b] Filament speeds shown with S.D. of actin filaments from *in vitro* motility assays ($n = 2$).
[c] The average values for the percent moving filaments and the total number of filaments ($n = 2$).

DISCUSSION

The present work relates functional analyses to computational models and reports significant progress toward our goal to establish the actin-Tm interface in the absence of an atomic resolution structure. Our goal in the present study was to determine the actin-tropomyosin interface residues in the absence of proteins such as troponin and myosin that modify the intrinsic actin affinity of tropomyosin. We have defined common features of the interface while gaining insight into period-specific features of actin binding sites on Tm. The current work builds on our previous analysis of evolutionarily conserved sites. Here, we included periods P1 and P7 and mutated additional conserved sites in the first half of P2–P6 that are well conserved but

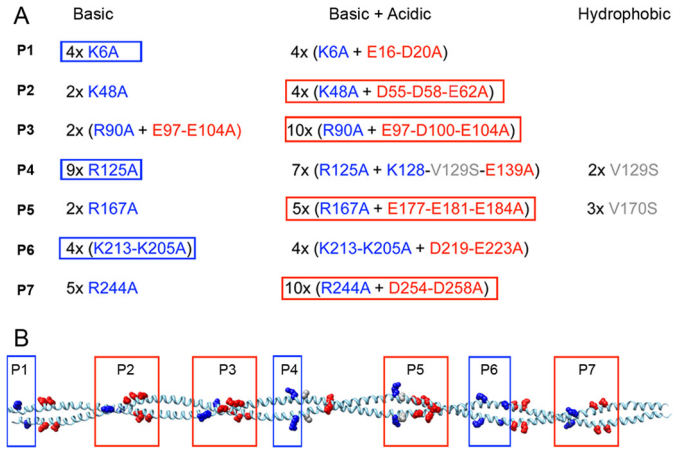

FIGURE 6. **Summary of contributions of basic, acidic, and hydrophobic residues in individual periodic repeats to tropomyosin function.** *A*, tropomyosin residues at conserved surface positions that were mutated to Ala in the first half of periods P1–P7 (basic residues in *blue*, acidic residues in *red*, and hydrophobic residues in *gray*). The *numbers* indicate the reduction in actin affinity of the mutants compared with WT Tm (K_{WT}/K_{mut}). In P1, P4, and P6, primarily basic residues contribute to actin affinity (*blue boxes*), in contrast to P2, P3, P5, and P7, where both basic and acidic or mostly acidic residues contribute to actin affinity (*red boxes*). The hydrophobic residues have a smaller contribution to actin affinity. *B*, tropomyosin mutations shown in the 7 Å striated muscle αTm structure (Protein Data Bank code 1C1G) (49).

that fell above the arbitrary cutoff of $\omega \leq 0.015$ in our previous study (20).

An earlier model of the periodic repeats identified a pattern of seven conserved surface residues proposed to be actin binding sites (7) that has been tested and supported (10, 11). Of these seven residues, a basic residue in an *f* position at the beginning of the repeat, followed by acidic residues in *b* and *f* postions in an *i* to *i* + *4* relationship, are the most consistent features of the repeat (Fig. 1) and are shown to be important in our iterative analyses. Here, we show that the basic residue participates in all seven sites with an alternating pattern of sites with basic (P1, P4, P6) and basic-acidic residues (P2, P3, P5, P7) (Fig. 6). The results underscore previous reports of particular contributions of each period to actin affinity and thin filament function (11–15). The relatively minor involvement of hydrophobic residues is consistent with the primarily electrostatic nature of actin-Tm binding. Without an atomic resolution structure, however, our present proposal does not preclude the involvement of additional residues in the actin-Tm interface.

We note that the basic and basic-acidic motifs of the proposed actin binding sites include non-canonical features of the Tm coiled coil interface that are themselves highly conserved and may therefore be crucial for local conformation and interaction with actin. P1 and P5 have "alanine clusters" that cause local flexibility (21, 34), a feature important for actin affinity (9–11). Two highly conserved non-canonical interface residues (Asp^{137} in a *d* position and Glu^{218} in an *a* position) that cause bends in the molecule (21, 35, 36), are in P4 and P6, respectively.

Our finding that Tm fails to bind to actin mutated at Asp^{25}-Glu^{334}-Lys^{326}-Lys^{328} supports the available molecular models for actin-Tm in the closed state (18, 20, 21). Therefore, one or more of the four mutated actin residues are binding sites for Tm. The slight (~25%) inhibition of velocity of the actin mutant relative to WT actin in the motility assay also indicates

the involvement of the mutated residues in myosin binding or ATPase activation. Atomic models of actin-myosin show actin residues Lys^{326} and Glu^{334} as myosin binding residues (16, 37). The hypothesis that Tm and myosin compete for a common site on actin in the steric blocking model (38–41) is supported by the reduced velocity of filament speed in an actin-myosin motility assay.

In summary, the binding sites of Tm and actin based on our mutagenesis studies support atomic models of actin-Tm (18, 20, 21), where in the absence of troponin and myosin, Tm is predicted to bind to the actin filament at subdomains 1 and 3 and inhibit the binding of myosin to actin. Three sites in the pattern of basic-acidic residues in Tm, Glu^{62} in P2, Arg^{167} in P5, and Arg^{244} in P7, are the sites of disease-causing mutations in humans (4, 5). Some of the actin mutations studied here are also known to be disease-causing mutations in the human skeletal muscle actin gene (*ACTA1*) (42) are lethal in yeast and cause abnormal muscle structure in *Caenorhabditis* and *Drosophila* (43–46). It is likely that severely impaired binding of Tm to actin filaments may explain these phenotypes.

Acknowledgments—We thank Brinda Desai and Yazan Alkhawam for technical assistance.

REFERENCES

1. Gunning, P., O'Neill, G., and Hardeman, E. (2008) Tropomyosin-based regulation of the actin cytoskeleton in time and space. *Physiol. Rev.* **88,** 1–35
2. Pollard, T. D., and Cooper, J. A. (2009) Actin, a central player in cell shape and movement. *Science* **326,** 1208–1212
3. Wang, C. L., and Coluccio, L. M. (2010) New insights into the regulation of the actin cytoskeleton by tropomyosin. *Int. Rev. Cell Mol. Biol.* **281,** 91–128
4. Kee, A. J., and Hardeman, E. C. (2008) Tropomyosins in skeletal muscle diseases. *Adv. Exp. Med. Biol.* **644,** 143–157
5. Wieczorek, D. F., Jagatheesan, G., and Rajan, S. (2008) The role of tropomyosin in heart disease. *Adv. Exp. Med. Biol.* **644,** 132–142
6. McLachlan, A. D., and Stewart, M. (1976) The 14-fold periodicity in α-tropomyosin and the interaction with actin. *J. Mol. Biol.* **103,** 271–298
7. Phillips, G. N., Jr. (1986) Construction of an atomic model for tropomyosin and implications for interactions with actin. *J. Mol. Biol.* **192,** 128–131
8. Hitchcock-DeGregori, S. E. (2008) Tropomyosin: function follows structure. *Adv. Exp. Med. Biol.* **644,** 60–72
9. Singh, A., and Hitchcock-DeGregori, S. E. (2003) Local destabilization of the tropomyosin coiled coil gives the molecular flexibility required for actin binding. *Biochemistry* **42,** 14114–14121
10. Singh, A., and Hitchcock-DeGregori, S. E. (2006) Dual requirement for flexibility and specificity for binding of the coiled-coil tropomyosin to its target, actin. *Structure* **14,** 43–50
11. Singh, A., and Hitchcock-DeGregori, S. E. (2007) Tropomyosin's periods are quasi-equivalent for actin binding but have specific regulatory functions. *Biochemistry* **46,** 14917–14927
12. Landis, C., Back, N., Homsher, E., and Tobacman, L. S. (1999) Effects of tropomyosin internal deletions on thin filament function. *J. Biol. Chem.* **274,** 31279–31285
13. Hitchcock-DeGregori, S. E., Song, Y., and Greenfield, N. J. (2002) Functions of tropomyosin's periodic repeats. *Biochemistry* **41,** 15036–15044
14. Kawai, M., Lu, X., Hitchcock-Degregori, S. E., Stanton, K. J., and Wandling, M. W. (2009) Tropomyosin period 3 is essential for enhancement of isometric tension in thin filament-reconstituted bovine myocardium. *J. Biophys.* **2009,** 380967
15. Singh, A., and Hitchcock-Degregori, S. E. (2009) A peek into tropomyosin binding and unfolding on the actin filament. *PLoS One* **4,** e6336
16. Behrmann, E., Müller, M., Penczek, P. A., Mannherz, H. G., Manstein, D. J., and Raunser, S. (2012) Structure of the rigor actin-tropomyosin-Myosin complex. *Cell* **150,** 327–338
17. Lehman, W., and Craig, R. (2008) Tropomyosin and the steric mechanism of muscle regulation. *Adv. Exp. Med. Biol.* **644,** 95–109
18. Li, X. E., Tobacman, L. S., Mun, J. Y., Craig, R., Fischer, S., and Lehman, W. (2011) Tropomyosin position on F-actin revealed by EM reconstruction and computational chemistry. *Biophys. J.* **100,** 1005–1013
19. Miki, M., Makimura, S., Saitoh, T., Bunya, M., Sugahara, Y., Ueno, Y., Kimura-Sakiyama, C., and Tobita, H. (2011) A three-dimensional FRET analysis to construct an atomic model of the actin-tropomyosin complex on a reconstituted thin filament. *J. Mol. Biol.* **414,** 765–782
20. Barua, B., Pamula, M. C., and Hitchcock-DeGregori, S. E. (2011) Evolutionarily conserved surface residues constitute actin binding sites of tropomyosin. *Proc. Natl. Acad. Sci. U.S.A.* **108,** 10150–10155
21. Brown, J. H., Zhou, Z., Reshetnikova, L., Robinson, H., Yammani, R. D., Tobacman, L. S., and Cohen, C. (2005) Structure of the mid-region of tropomyosin: bending and binding sites for actin. *Proc. Natl. Acad. Sci. U.S.A.* **102,** 18878–18883
22. Barua, B., Winkelmann, D. A., White, H. D., and Hitchcock-DeGregori, S. E. (2012) Regulation of actin-myosin interaction by conserved periodic sites of tropomyosin. *Proc. Natl. Acad. Sci. U.S.A.* **109,** 18425–18430
23. Monteiro, P. B., Lataro, R. C., Ferro, J. A., and Reinach Fde, C. (1994) Functional α-tropomyosin produced in *Escherichia coli*. A dipeptide extension can substitute the amino-terminal acetyl group. *J. Biol. Chem.* **269,** 10461–10466
24. Hitchcock-De Gregori, S. E., Mandala, S., and Sachs, G. A. (1982) Changes in actin lysine reactivities during polymerization detected using a competitive labeling method. *J. Biol. Chem.* **257,** 12573–12580
25. O'Reilly, D. R., Miller, L.K., and Luckow, V.A. (1992) *Baculovirus Expression Vectors, A Laboratory Manual*, W.H. Freeman and Co., New York
26. Noguchi, T. Q., Gomibuchi, Y., Murakami, K., Ueno, H., Hirose, K., Wakabayashi, T., and Uyeda, T. Q. (2010) Dominant negative mutant actins identified in flightless *Drosophila* can be classified into three classes. *J. Biol. Chem.* **285,** 4337–4347
27. Hammell, R. L., and Hitchcock-DeGregori, S. E. (1996) Mapping the functional domains within the carboxyl terminus of α-tropomyosin encoded by the alternatively spliced ninth exon. *J. Biol. Chem.* **271,** 4236–4242
28. Greenfield, N. J., and Hitchcock-DeGregori, S. E. (1995) The stability of tropomyosin, a two-stranded coiled-coil protein, is primarily a function of the hydrophobicity of residues at the helix-helix interface. *Biochemistry* **34,** 16797–16805
29. Winkelmann, D. A., Bourdieu, L., Ott, A., Kinose, F., and Libchaber, A. (1995) Flexibility of myosin attachment to surfaces influences F-actin motion. *Biophys. J.* **68,** 2444–2453
30. Bourdieu, L., Magnasco, M. O., Winkelmann, D. A., and Libchaber, A. (1995) Actin filaments on myosin beds: The velocity distribution. *Phys. Rev. E Stat. Phys. Plasmas Fluids Relat. Interdiscip. Topics* **52,** 6573–6579
31. Wang, Q., Moncman, C. L., and Winkelmann, D. A. (2003) Mutations in the motor domain modulate myosin activity and myofibril organization. *J. Cell Sci.* **116,** 4227–4238
32. Lu, X., Tobacman, L. S., and Kawai, M. (2003) Effects of tropomyosin internal deletion Δ23Tm on isometric tension and the cross-bridge kinetics in bovine myocardium. *J. Physiol.* **553,** 457–471
33. Lu, X., Tobacman, L. S., and Kawai, M. (2006) Temperature-dependence of isometric tension and cross-bridge kinetics of cardiac muscle fibers reconstituted with a tropomyosin internal deletion mutant. *Biophys. J.* **91,** 4230–4240
34. Brown, J. H., Kim, K. H., Jun, G., Greenfield, N. J., Dominguez, R., Volkmann, N., Hitchcock-DeGregori, S. E., and Cohen, C. (2001) Deciphering the design of the tropomyosin molecule. *Proc. Natl. Acad. Sci. U.S.A.* **98,** 8496–8501
35. Nitanai, Y., Minakata, S., Maeda, K., Oda, N., and Maéda, Y. (2007) Crystal structures of tropomyosin: flexible coiled-coil. *Adv. Exp. Med. Biol.* **592,** 137–151
36. Sumida, J. P., Wu, E., and Lehrer, S. S. (2008) Conserved Asp-137 imparts flexibility to tropomyosin and affects function. *J. Biol. Chem.* **283,** 6728–6734

37. Lorenz, M., and Holmes, K. C. (2010) The actin-myosin interface. *Proc. Natl. Acad. Sci. U.S.A.* **107,** 12529–12534
38. Haselgrove, J. C. (1972) X-ray evidence for a conformational change in the actin-containing filaments of vertebrate striated muscle. *Cold Spring Harbor Symp. Quant. Biol.* **37,** 341–352
39. Huxley, H. E. (1972) Structural changes in actin and myosin-containing filaments during contraction. *Cold Spring Harbor Symp. Quant. Biol.* **37,** 361–376
40. Parry, D. A., and Squire, J. M. (1973) Structural role of tropomyosin in muscle regulation: analysis of the x-ray diffraction patterns from relaxed and contracting muscles. *J. Mol. Biol.* **75,** 33–55
41. Vibert, P., Craig, R., and Lehman, W. (1997) Steric-model for activation of muscle thin filaments. *J. Mol. Biol.* **266,** 8–14
42. Laing, N. G., Dye, D. E., Wallgren-Pettersson, C., Richard, G., Monnier, N., Lillis, S., Winder, T. L., Lochmüller, H., Graziano, C., Mitrani-Rosenbaum, S., Twomey, D., Sparrow, J. C., Beggs, A. H., and Nowak, K. J. (2009) Mutations and polymorphisms of the skeletal muscle α-actin gene (ACTA1). *Hum. Mutat.* **30,** 1267–1277
43. Drummond, D. R., Hennessey, E. S., and Sparrow, J. C. (1991) Characterisation of missense mutations in the Act88F gene of *Drosophila melanogaster*. *Mol. Gen. Genet.* **226,** 70–80
44. Frieden, C., Du, J., Schriefer, L., and Buzan, J. (2000) Purification and polymerization properties of two lethal yeast actin mutants. *Biochem. Biophys. Res. Commun.* **271,** 464–468
45. Waterston, R. H., Hirsh, D., and Lane, T. R. (1984) Dominant mutations affecting muscle structure in *Caenorhabditis elegans* that map near the actin gene cluster. *J. Mol. Biol.* **180,** 473–496
46. Wertman, K. F., Drubin, D. G., and Botstein, D. (1992) Systematic mutational analysis of the yeast ACT1 gene. *Genetics* **132,** 337–350
47. Fujii, T., Iwane, A. H., Yanagida, T., and Namba, K. (2010) Direct visualization of secondary structures of F-actin by electron cryomicroscopy. *Nature* **467,** 724–728
48. Pettersen, E. F., Goddard, T. D., Huang, C. C., Couch, G. S., Greenblatt, D. M., Meng, E. C., and Ferrin, T. E. (2004) UCSF Chimera–a visualization system for exploratory research and analysis. *J. Comput. Chem.* **25,** 1605–1612
49. Whitby, F. G., and Phillips, G. N., Jr. (2000) Crystal structure of tropomyosin at 7 Angstroms resolution. *Proteins* **38,** 49–59